

The effect of viscosity and diffusion on the HO₂ uptake by sucrose and secondary organic aerosol particles

Pascale S. J. Lakey^{1,2}, Thomas Berkemeier², Manuel Krapf³, Josef Dommen³, Sarah S. Steimer³, Lisa K. Whalley^{1,4}, Trevor Ingham^{1,4}, Maria T. Baeza-Romero⁵, Ulrich Pöschl², Manabu Shiraiwa^{2,6}, Markus Ammann³ and Dwayne E. Heard^{1,4,*}

¹ School of Chemistry, University of Leeds, Woodhouse Lane, Leeds, LS2 9JT, UK

² Multiphase Chemistry Department, Max-Planck-Institute for Chemistry, Hahn-Meitner-Weg 1, 55128 Mainz, Germany.

³ Paul Scherrer Institute, Villigen, Switzerland.

⁴ National Centre for Atmospheric Chemistry, University of Leeds, Woodhouse Lane, Leeds, LS2 9JT, UK

⁵ Escuela de Ingeniería Industrial de Toledo, Universidad de Castilla la Mancha, Avenida Carlos III s/n Real Fábrica de Armas, Toledo, 45071, Spain

⁶ Department of Chemistry, University of California Irvine, CA 92617, United States

* Corresponding author: Dwayne Heard (D.E.Heard@leeds.ac.uk)

Abstract

We report the first measurements of HO₂ uptake coefficients, γ , for secondary organic aerosol particles (SOA) and for the well-studied model compound sucrose which we doped with copper (II). Above 65% relative humidity (RH), γ for copper (II) doped sucrose aerosol particles equalled the surface mass accommodation coefficient $\alpha = 0.22 \pm 0.06$ but decreased to $\gamma = 0.012 \pm 0.007$ upon decreasing the RH to 17%. The trend of γ with RH can be explained by an increase in aerosol viscosity and the contribution of a surface reaction, as demonstrated using the kinetic multi-layer model of aerosol surface and bulk chemistry (KM-SUB). At high RH the total uptake was driven by reaction in the near-surface bulk limited by mass accommodation whilst at low RH it was limited by surface reaction. SOA from two different precursors, α -pinene and 1,3,5-trimethylbenzene (TMB), was investigated, yielding low uptake coefficients of $\gamma < 0.001$ and $\gamma = 0.004 \pm 0.002$, respectively. It is postulated that the larger values measured for TMB derived SOA compared to α -pinene derived SOA are either due to differing

32 viscosity, a different liquid water content of the aerosol particles or a $\text{HO}_2 + \text{RO}_2$ reaction occurring
33 within the aerosol particles.

34 **Introduction**

35

36 OH and HO_2 radicals play a vital role in atmospheric chemistry by controlling the oxidative
37 capacity of the troposphere, with HO_2 acting as a short-lived reservoir for OH. Oxidation by the OH
38 radical determines the lifetime and concentrations of many trace gases within the troposphere such as
39 NO_x (NO and NO_2), CH_4 and volatile organic compounds (VOCs). The reaction of HO_2 with NO also
40 constitutes an important source of ozone, which is damaging to plants, a respiratory irritant and a
41 greenhouse gas (Pöschl and Shiraiwa, 2015;Fowler et al., 2009). It is therefore important to have a
42 thorough understanding of the reactions and processes that affect HO_x concentrations. However, during
43 field campaigns HO_2 concentrations have sometimes been measured as being lower than the
44 concentrations predicted by constrained box models implying a missing HO_2 sink, which has often been
45 attributed to HO_2 uptake by aerosol particles (e.g. (Kanaya et al., 2007;Mao et al., 2010;Whalley et al.,
46 2010)).

47 SOA is generated from low-volatility products formed by the oxidation of VOCs, and it
48 accounts for a large fraction of the organic matter in the troposphere. For example, in urban areas it can
49 account for up to 90 % of the organic particulate mass (Kanakidou et al., 2005;Lim and Turpin, 2002).
50 Lakey et al. (2015a) previously measured the HO_2 uptake coefficient onto single component organic
51 aerosol particles as ranging from $\gamma < 0.004$ to $\gamma = 0.008 \pm 0.004$ unless elevated transition metal ions,
52 that catalyse the destruction of HO_2 , were present within the aerosol. Taketani et al. (2013) and Taketani
53 and Kanaya (2010) also measured the HO_2 uptake coefficient onto dicarboxylic acids ($\gamma = 0.02 \pm 0.01$
54 to $\gamma = 0.18 \pm 0.07$) and levoglucosan ($\gamma < 0.01$ to $\gamma = 0.13 \pm 0.03$) over a range of humidities. However,
55 there are currently no measurements of the HO_2 uptake coefficient onto SOA published in the literature.

56 Using the kinetic multi-layer model of aerosol surface and bulk chemistry (KM-SUB), Shiraiwa
57 et al. (2011b) have shown that the bulk diffusion of a species within an aerosol matrix can have a large
58 impact on a measured uptake coefficient. Diffusion coefficients of a particular species within a particle
59 are related to the viscosity of that particle with larger diffusion coefficients in less viscous particles.
60 Traditionally, the relationship between viscosity and diffusion coefficients is given by the Stokes-
61 Einstein equation, although this relation was found to break down for concentrated solutions and
62 solutions near their glass transition temperature or humidity (Champion et al., 1997;Power et al., 2013).
63 Zhou et al. (2013) have also shown that the rate of heterogeneous reaction of particle-borne
64 benzo[a]pyrene (BaP) with ozone within SOA particles was strongly dependent upon the bulk
65 diffusivity of the SOA. Along the same lines, Steimer et al. (2015) and Steimer et al. (2014)

66 demonstrated a clear link between the ozonolysis rates of shikimic acid and the changing diffusivity in
67 the transition between liquid and glassy states. Previous measurements of both N_2O_5 uptake coefficients
68 and HO_2 uptake coefficients onto humic acid aerosol particles and N_2O_5 uptake coefficients onto
69 malonic acid and citric acid aerosol particles have shown much lower uptake coefficients at low relative
70 humidities compared to higher humidities (Badger et al., 2006;Thornton et al., 2003;Lakey et al.,
71 2015a;Gržinić et al., 2015). However, viscosity effects have not been investigated systematically for
72 HO_2 uptake, and the first aim of this paper was to investigate whether a change in aerosol viscosity,
73 exemplified using the well-studied model compound sucrose (Berkemeier et al., 2014;Price et al.,
74 2014;Zobrist et al., 2011), could impact the HO_2 uptake coefficient. The second aim of this study was
75 to measure the HO_2 uptake coefficient onto two different types of SOA representative of biogenic and
76 anthropogenic SOA. α -pinene is the major terpene that forms biogenic SOA, while 1,3,5-
77 trimethylbenzene (TMB) is representative of alkyl benzenes which are the most abundant aromatic
78 hydrocarbons and form anthropogenic SOA (Calvert et al., 2002;Qi et al., 2012). SOA is known to be
79 highly viscous with viscosities of $10^3 - 10^6$ Pa s at 50 % RH (Renbaum-Wolff et al., 2013).

80

81 **Experimental**

82

83 The general experimental setup for the Leeds aerosol flow tube and the data analysis
84 methodology to determine values of γ have previously been discussed in detail by George et al. (2013).
85 This is the same experimental setup and data analysis methodology that was used for the copper (II)
86 doped sucrose experiments, which were also performed at the University of Leeds. Therefore, only a
87 brief description of the setup is included below, with the emphasis being on changes made to the
88 apparatus for the SOA experiments undertaken at the Paul Scherrer Institute (PSI), for which a
89 schematic is shown in Figure 1. For all experiments the HO_2 radical was released at the end of an
90 injector which was moved backwards and forwards along an aerosol flow tube. The flow from the
91 injector was 1.32 ± 0.05 slpm. For the copper doped sucrose experiments the humid aerosol flow was
92 1.0 ± 0.1 slpm, and was mixed with a much drier flow (with the humidity of this flow being controlled
93 by mixing a flow from a water bubbler with a dry flow in different ratios) of 3.0 ± 0.3 slpm within a
94 conditioning flow tube for approximately ten seconds before entering the aerosol flow tube. Nitrogen
95 was used for all of these flows. For the SOA experiments the flow from the smog chamber or Potential
96 Aerosol Mass (PAM) chamber at PSI was 4.0 ± 0.3 slpm. Decays of the HO_2 radical along an aerosol
97 flow tube were measured using a Fluorescence Assay by Gas Expansion (FAGE) detector in both the
98 absence and presence of different concentrations of aerosol particles. All experiments were performed
99 at room temperature (293 ± 2 K).

100 The HO₂ radical was formed via Reactions 1 – 2, by passing a humidified flow over a mercury penray
101 lamp (L.O.T. Oriel, model 6035) in the presence of trace amounts (20 – 30 ppm) of oxygen in the
102 nitrogen flow.

103



106

107 Data acquisition was only started once HO₂ concentrations within the flow tube were stable
108 which occurred within 1 minute of switching on the mercury lamp. The HO₂ radicals entered the FAGE
109 cell through a 0.7 mm diameter pinhole, and were then converted to OH by reacting with added NO.
110 The FAGE cell was either kept at a pressure of ~ 0.85 Torr or ~ 1.5 Torr using a combination of a rotary
111 pump (Edwards, model E1M80) and a roots blower (EH1200). The OH radicals were detected by laser
112 induced fluorescence at 308 nm (Heard and Pilling, 2003; Stone et al., 2012). Initial HO₂ concentrations
113 (obtained by calibration) exiting the injector were measured as ~ 1 × 10⁹ molecule cm⁻³ for all
114 experiments (following mixing and dilution with the main flow), and the concentration was then
115 measured as a function of distance along the flow tube.

116 For the experiments using copper doped sucrose aerosol particles, 3.42 grams of sucrose
117 (Fisher, > 99%) and 0.125 grams of copper (II) sulphate pentahydrate were dissolved in 500 ml of
118 milliQ water. These solutions were then placed in an atomiser (TSI, 3076) in order to form aerosol
119 particles. The aerosol particles passed through a neutraliser (Grimm 5522) and an impactor before
120 entering the conditioning flow tube. The size distribution of the aerosol particles were then measured
121 at the end of the reaction flow tube using a Scanning Mobility Particle Sizer (SMPS, TSI, 3080).

122 The experimental setup used to measure previous HO₂ uptake coefficients (George et al.,
123 2013; Matthews et al., 2014; Lakey et al., 2015a; Lakey et al., 2015b) was transported from the University
124 of Leeds, UK, to the Paul Scherrer Institute, Switzerland, where it was connected to the Paul Scherrer
125 Institute (PSI) smog chamber and, for some of the experiments, also to a Potential Aerosol Mass (PAM)
126 chamber (see Figure 1). The PSI smog chamber has a volume of 27 cubic metres, it is made from 125
127 μm Teflon fluorocarbon film and has been described elsewhere (Paulsen et al., 2005). To initiate
128 photochemical reactions four 4 kW xenon arc lamps (light spectrum >280 nm, OSRAM) and eighty
129 black lights (100W tubes, light spectrum between 320 and 400 nm, Cleo Performance) were used. For
130 most experiments the chamber was first humidified to 50% relative humidity, but for two experiments
131 this was increased to 80%, after which the precursor gases were added. The concept, design and
132 operation of a PAM chamber has also previously been described (Kang et al., 2007). The PAM chamber

133 at PSI is a flow tube of 0.46 m in length and 0.22 m internal diameter. Two low pressure Hg lamps
134 mainly emitting at 185 and 254 nm produce ozone in the chamber. Water vapour was photolysed by the
135 185 nm radiation to produce OH and HO₂ and also photolysed O₂ to produce O₃, whereas the 254 nm
136 light could also photolyse O₃ to produce OH following the reaction of O(¹D) with water vapour. Upper-
137 limit OH production rates are in the range of 1×10^{12} - 2×10^{12} molecule cm⁻³ s⁻¹ (Bruns et al., 2015).
138 The composition and oxidation state of SOA formed within PAM chambers has previously been shown
139 to be similar to SOA generated within environmental chambers (Bruns et al., 2015; Lambe et al., 2011a)
140 and SOA in the atmosphere (Ortega et al., 2015).

141 Four different types of experiments were performed.

142 (i) α -pinene ozonolysis in the PSI smog chamber (600 ppb α -pinene, 280 ppb ozone: ozone was added
143 first to the chamber; after injection of α -pinene particle nucleation and growth rapidly occurred).

144 (ii) OH initiated α -pinene photochemistry in the smog chamber (500 ppb α -pinene, 350 ppb NO₂: Xenon
145 and black lights were used to initiate photochemical reactions).

146 (iii) OH initiated α -pinene photochemistry in the PAM chamber (500 ppb α -pinene was filled into the
147 large smog chamber at 50 or 80 % RH to supply a constant concentration of α -pinene to the PAM
148 chamber, all SOA was formed within the PAM chamber).

149 (iv) OH initiated TMB photochemistry in the PAM chamber (2 ppm TMB was filled into the large smog
150 chamber at 50 % RH to supply a constant concentration of TMB to the PAM chamber, all SOA was
151 formed within the PAM chamber).

152 These precursor concentrations were chosen in order to obtain a large enough aerosol surface
153 area in the flow tube to be able to measure a HO₂ uptake coefficient. Experiments were performed only
154 once the aerosol surface area within the aerosol flow tube exceeded 5×10^{-5} cm² cm⁻³, and in the case
155 of the smog chamber experiments once a maximum aerosol concentration had been reached (as
156 summarised in the Results Section). Prior to entering the flow tube, the aerosol flow from the smog or
157 PAM chamber (4.0 slpm) was passed through either two or three cobalt oxide denuders in series (each
158 40 cm long, 0.8 cm inner diameter quartz tubes coated with cobalt oxide prepared by thermal
159 decomposition of a saturated Co(NO₃)₂ solution applied to its inner walls at 700°C as described in
160 Ammann (2001)), which in turn were in series with a charcoal denuder (length = 16.4 cm, diameter =
161 0.9 cm, 69 quadratic channels) in order to remove NO_x species, RO₂, VOC's and ozone that had been
162 present in the chamber. These denuders have previously been shown to be extremely efficient at
163 removing gas phase NO_x and VOCs (Arens et al., 2001). It should be noted that the flows were drawn
164 through the aerosol flow tube using a pump instead of the normal procedure whereby the flows are
165 pushed through the experimental setup using mass flow controllers. The pumping setup led to slightly

166 reduced pressures (904 – 987 mbar) in the aerosol flow tube, and so careful checks were performed to
167 ensure that the flow tube was vacuum tight. The aerosol size distribution from which the surface area
168 exiting the flow tube was calculated was measured using a Scanning Mobility Particle Sizer (SMPS),
169 which consisted of a neutraliser (Kr-85), a Differential Mobility Analyser (DMA, length 93.5 cm, inner
170 radius 0.937 cm and outer radius 1.961 cm) and a CPC (TSI, model 3022). A typical surface weighted
171 aerosol size distribution for the α -pinene derived aerosol particles is shown in Figure 2. Note that an
172 impactor was not used in the experimental setup for the SOA measurements as this restricted the flow
173 that could be pumped through the flow tube and was also found to be unnecessary as the aerosol size
174 distribution from the chambers fell entirely within the range of aerosol sizes that the SMPS could
175 measure.

176 In order to check that the experimental setup used at PSI produced consistent results with those
177 previously performed at the University of Leeds, an experiment was performed with ammonium
178 sulphate aerosol particles. The ammonium sulphate aerosol particles were formed using an atomiser
179 rather than aerosol particles being formed in a chamber, but were then passed through the same set up
180 (including the denuders) as the SOA was passed through. The experiment was performed at a flow tube
181 pressure of 915 mbar, due to the flows being pumped through the setup, (compared to pressures of 904
182 – 987 mbar for the SOA experiments), and a HO₂ uptake coefficient of 0.004 ± 0.002 was measured at
183 60% RH which is in agreement with previous experiments by George et al. (2013), which were
184 performed at atmospheric pressure (~ 970 – 1040 mbar).

185

186 **Data analysis**

187

188 Experiments were performed by moving the HO₂ injector backwards and forwards along the
189 flow tube either in the presence of or in the absence of aerosol particles, and recording the FAGE signal
190 from HO₂ radicals. The background signal in the absence of HO₂ (mercury lamp in the injector switched
191 off), but with the NO entering the FAGE cell, was recorded and was subtracted, from the signal during
192 experiments. For α -pinene experiments this background signal was small and similar to previous
193 experiments using dust, organic and inorganic salt aerosol particles (George et al., 2013;Lakey et al.,
194 2015b;Lakey et al., 2015a;Matthews et al., 2014). However, for the TMB experiments this background
195 signal varied from about half to two thirds of the signal from HO₂ with the mercury lamp in the injector
196 switched on. The background signal disappeared when the NO added to the FAGE cell was switched
197 off showing that it was not due to OH. The background signal within experiments did not change when
198 aerosol particles were present compared to when they were completely filtered out (see Figure 1).
199 Although the denuders are efficient at removing gas phase species (Arens et al., 2001), it can be

200 hypothesized that the signal was due to the formation of HO₂ and RO₂ radicals generated by a small
 201 fraction of ozone, precursors and oxidation products passing through the denuders for the TMB
 202 experiments. RO₂ species would have been observed as a HO₂ interference by the FAGE detection
 203 method. FAGE interferences have previously been observed for alkene, aromatic and > C₃ alkane
 204 derived RO₂ (Fuchs et al., 2011; Whalley et al., 2013). A box model was run, utilising chemistry within
 205 the Master Chemical Mechanism (MCM 3.2), which is detailed further in Whalley et al. (2013)), and
 206 constrained to the experimental concentrations, and showed that the expected interference from TMB
 207 RO₂ and α -pinene RO₂ would have been equivalent to $0.59 \times [\text{HO}_2]$ and $0.44 \times [\text{HO}_2]$, respectively, at
 208 a NO flow of 50 ml min⁻¹ into the FAGE cell, a FAGE pressure of 1.5 Torr and a flow through the
 209 FAGE pinhole of 4.2 slpm. However, for α -pinene experiments the background signal did not change
 210 between the NO being switched on and off with the mercury lamp switched off in the injector, indicating
 211 the absence of interferences in the FAGE cell for these experiments. The lack of interference for the α -
 212 pinene experiments suggests that the denuders were more efficient at removing the gas phase precursors
 213 and oxidation products from the chamber and that only negligible concentrations of RO₂ species were
 214 present in the flow tube. Nevertheless, since for the TMB experiments a significant background signal
 215 was observed, that signal was measured regularly throughout the experiment and used to correct the
 216 measurement data.

217 HO₂ decays along the flow tube in the presence and absence of aerosol particles were measured
 218 between ~ 10 and 18 seconds flow time after the point of injection to ensure thorough mixing. A
 219 previous calculation showed that the flows should be fully mixed by ~ 7 seconds (George et al., 2013).
 220 An example of the HO₂ decays in the presence and absence of aerosol particles for a TMB experiment
 221 is shown in Figure 3, plotted as the natural logarithm of HO₂ signal (proportional to concentration)
 222 against reaction time according to:

$$223 \quad \ln \frac{[\text{HO}_2]_t}{[\text{HO}_2]_0} = -k_{obs}t \quad (\text{E1})$$

224 There is clear uptake of HO₂ observed by the SOA derived from TMB. The pseudo first-order
 225 rate coefficients (k_{obs}) were then corrected for wall losses and non-plug flow conditions using the
 226 methodology described by Brown (1978). The average correction was 22%. These corrected rate
 constants (k') were related to the HO₂ uptake coefficient (γ_{obs}) by the following equation:

$$227 \quad k' = \frac{\gamma_{obs}\omega_{HO_2}S}{4} \quad (\text{E2})$$

228 where ω_{HO_2} is the molecular thermal speed of HO₂ and S is the total aerosol surface area. Examples of
 229 k' as a function of the aerosol surface area is shown in Figure 4. The HO₂ uptake coefficients were then
 230 corrected for gas-phase diffusion limitations using the methodology described by (Fuchs and Sutugin,
 1970), although this correction changed the uptake coefficient by less than 1 % for all experiments.

231

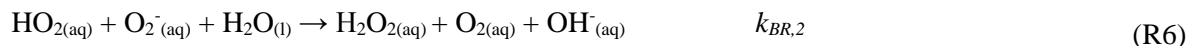
232 **Model description**

233

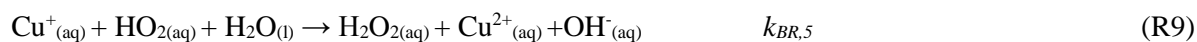
234 The kinetic multi-layer model of aerosol surface and bulk chemistry (KM-SUB) has been
 235 described in detail by Shiraiwa et al. (2010). It is a multi-layer model comprising a gas phase, a near-
 236 surface gas phase, a sorption layer, a near-surface bulk layer and a number of bulk layers arranged in
 237 spherical geometry. Processes that can occur within the model include gas-phase diffusion, adsorption
 238 and desorption, bulk diffusion, and chemical reactions in the gas phase, at the surface and in the bulk.
 239 In contrast to traditional resistor models, the KM-SUB model enables efficient treatment of complex
 240 chemical mechanisms. Input parameters to the model are summarised in Table 1 whilst the reactions
 241 that were included are shown below:



242



243



244

245 The bulk layer number was set to 100 corresponding to a bulk layer thickness of 0.5 nm which
 246 is only slightly larger than the diameter of HO₂ (0.4 nm) and implies that HO₂ only needs to travel
 247 approximately the distance of its own diameter to go from being an adsorbed radical on the surface of
 248 the aerosol particle to a dissolved aqueous radical. The same short distance must be overcome by HO₂
 249 to move between bulk layers, which is important for convergence of the numerical model, especially
 250 when the chemical reactions within the aerosol particles are very fast compared to the diffusion time
 251 scales, leading to steep concentration gradients within the particle. Reducing the bulk layer thickness
 252 further did not significantly impact the calculated uptake coefficients.

253 During experiments the average radius was observed to change by less than 10 % over the range
254 of humidities, and therefore an assumption was made within the model that the average aerosol radius
255 remained constant over the range of relative humidities. For the diffusion coefficient of HO₂ within
256 aerosol particles we used the measured diffusion coefficients of H₂O within sucrose solutions, which
257 we then corrected using the Stokes-Einstein equation to take into account the larger radius of HO₂
258 radicals compared to H₂O molecules (Price et al., 2014; Zobrist et al., 2011). The correction resulted in
259 a factor of 1.22 decrease in the diffusion coefficients of HO₂ compared to the diffusion coefficients of
260 H₂O. It should be noted that above a viscosity of 10 Pa s the Stokes-Einstein relationship starts to fail
261 and that the effect of increasing molecular size may become much stronger (Power et al., 2013). Price
262 et al. (2014) estimated diffusion coefficients of H₂O by using Raman spectroscopy to observe D₂O
263 diffusion in high-viscosity sucrose solutions whilst Zobrist et al. (2011) used optical techniques to
264 observe changes in the size of sucrose particles when exposed to different relative humidities.

265 Sensitivity tests showed that the diffusion rate constants of O₂⁻, Cu⁺ and Cu²⁺ did not influence
266 calculation results. The reaction rate coefficients involving copper (k_{BR,3} - k_{BR,6}) are so large that O₂⁻ is
267 produced *in situ* and consumed locally. The catalytic nature of these reactions cause Cu⁺ and Cu²⁺ to
268 rapidly interconvert meaning that they remain available at high concentrations in the upper layers of the
269 aerosol particle. Similarly, as sucrose does not react with any species within the model, its diffusion
270 within the model is unimportant to the outputted HO₂ uptake coefficient.

271

272 **Results and Discussion**

273

274 **HO₂ uptake by copper doped sucrose aerosol particles**

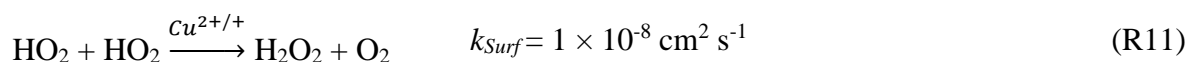
275

276 The results of the HO₂ uptake coefficient measurements onto copper doped sucrose aerosol
277 particles as a function of relative humidity (RH) are shown in Figure 5. The results show a large
278 dependence upon relative humidity with the HO₂ uptake coefficient increasing from 0.012 ± 0.007 at
279 17 ± 2 % RH to 0.22 ± 0.06 at relative humidities above 65%. The latter value is likely equal to the
280 surface accommodation coefficient, and is consistent with many previous studies (Takahama and
281 Russell, 2011; George et al., 2013; Lakey et al., 2015b). At lower humidities, the diffusion coefficients
282 decrease which leads to slower transport of HO₂ within the bulk, and therefore to a slower overall rate
283 of HO₂ destruction (Reactions 7 – 10). The HO₂ reacto-diffusive length (Hanson et al., 1994; Schwartz
284 and Freiberg, 1981) varied from between ~ 4 – 7 nm at the highest relative humidity that was used (71
285 % RH) down to ~0.006 – 0.05 nm at the lowest relative humidity (17 % RH). The range of values for
286 the reacto-diffusive length at a given RH is due to the difference between the parameterizations of the

287 diffusion coefficient in Price et al. (2014) and Zobrist et al. (2011). These reacto-diffusive lengths
288 indicate that at all relative humidities HO₂ radicals will be limited to the outermost molecular layers of
289 the particle before reacting away, which is in agreement with the model. Note that it was shown in
290 previously that the uptake of gas-phase species generally increases with increasing reacto-diffusive
291 length, which is consistent with our HO₂ uptake coefficient measurements (Slade and Knopf,
292 2014; Davies and Wilson, 2015; Houle et al., 2015). The red and blue lines in Figure 5 show the predicted
293 HO₂ uptake coefficients using the KM-SUB model when using two different parameterisations for HO₂
294 diffusion coefficients as a function of RH (see the model description). There is good agreement between
295 the model and the measurements suggesting that the change in HO₂ uptake over the range of humidities
296 is indeed due to a change in the HO₂ diffusion coefficient which is in turn due to a change in the viscosity
297 of the aerosol particles. Sensitivity tests showed that an increase in the rate constants of reactions R7 –
298 R10 does not affect the HO₂ uptake coefficient. A two order of magnitude decrease in the rate constants
299 affects the uptake coefficient marginally by reducing it by less than 10 % in the 40 – 55 % relative
300 humidity range, but has no impact at the lower or higher relative humidities.

301 Using the kinetic framework and classification scheme of Berkemeier et al. (2013), Figure 6
302 illustrates how the change in relative humidity leads to a change in the kinetic regime of HO₂ uptake.
303 At the highest relative humidities the uptake is limited by surface accommodation. At intermediate
304 relative humidities with $\gamma < \alpha_{s,o}$, the uptake is limited by surface-to-bulk transport, which is related to
305 both solubility (Henry's law coefficient) and diffusivity (diffusion coefficient) in the kinetic model.
306 Under both conditions, the uptake is driven by chemical reaction in the near-surface bulk and effectively
307 limited by mass accommodation, which includes both surface accommodation and surface-to-bulk
308 transport (Behr et al., 2009; Berkemeier et al., 2013). At low relative humidities the HO₂ uptake
309 coefficient was limited by chemical reaction at the surface as discussed below (Berkemeier et al., 2013).

310 Although the viscosity changes by more than 8 orders of magnitude and the diffusion
311 coefficients change by 5-7 orders of magnitude over the investigated range of relative humidity, the
312 measured HO₂ uptake coefficients change by only ~ 1 order of magnitude. This can be explained to
313 some extent by the uptake coefficient being proportional to the square root of the diffusion coefficient
314 when the uptake is controlled by reaction and diffusion of HO₂ in the bulk (Davidovits et al.,
315 2006; Berkemeier et al., 2013). If this were the only mechanism involved, however, one would still
316 expect a change in the uptake coefficient by 2.5 – 3.5 orders of magnitude. The most plausible
317 explanation for the relatively high HO₂ uptake coefficients observed at low relative humidities is a
318 surface reaction of HO₂. For example, at 17 % RH and without a surface reaction, γ values as low as ~5
319 $\times 10^{-4}$ and ~3 $\times 10^{-5}$ would be expected using the Zobrist et al. (2011) and Price et al. (2014)
320 parameterisations, respectively. However, by including the following self-reaction of HO₂ at the surface
321 of the sucrose particles, much better agreement with the observed values of around ~10⁻² could be
322 obtained (Fig. 5):



324 Although the true mechanism for reaction at the surface remains unclear, the large rate constant for this
 325 reaction suggests that copper could potentially be catalyzing the destruction of HO₂ at the surface of the
 326 sucrose particles which is consistent with the higher HO₂ uptake coefficients measured onto solid
 327 aerosol particles containing transition metals compared to solid aerosol particles containing no
 328 transition metal ions (Matthews et al., 2014; Lakey et al., 2015a; Bedjanian et al., 2013; George et al.,
 329 2013). Note however that for a relevant surface reaction in kinetic flux models, it is necessary to use an
 330 effective desorption lifetime τ_d in the millisecond to second time range (Berkemeier et al.,
 331 2016; Shiraiwa et al., 2010). This is many orders of magnitude longer than would be expected due to
 332 pure physisorption as estimated by molecular dynamic simulations (Vieceli et al., 2005), indicating that
 333 the adsorption process should involve chemisorption or formation of long-lived intermediates that
 334 would have the potential to extend these effective desorption lifetimes (Shiraiwa et al.,
 335 2011a; Berkemeier et al., 2016). The effect and importance of surface reactions is consistent with
 336 previous work by Gržinić et al. (2015), Steimer et al. (2015) and Berkemeier et al. (2016) for the uptake
 337 of N₂O₅ to citric acid and the uptake of O₃ to shikimic acid over a range of relative humidities. A second
 338 potential reason for the discrepancy at low humidities could be an incomplete equilibration of the
 339 aerosol particles with respect to RH, as they had only been mixed with the conditioning flow for ~ 10
 340 seconds before entering the reaction flow tube. Bones et al. (2012) inferred from measurements on
 341 larger particles that for 100 nm diameter sucrose aerosol particles the equilibration time would be more
 342 than 10 seconds when the viscosity increased above ~ 10⁵ Pa s, which would occur at ~ 43 % RH (Power
 343 et al., 2013). The actual diffusion coefficients would thus be higher than assumed in calculations which
 344 assume fully equilibrated particles. However, the near-surface bulk of the aerosol particles, where the
 345 reactions occur, would be much better equilibrated with respect to RH than the inner core of the aerosol
 346 particles (Berkemeier et al., 2014). This means that the lack of aerosol equilibration with respect to RH
 347 is likely to have a negligible impact upon the HO₂ uptake coefficient.

348 It should also be noted that the KM-SUB modelling results were very sensitive to the initial
 349 aerosol pH. For example, at a pH of 4.1 (used in Figure 5, the reason for this value is discussed below)
 350 the HO₂ uptake coefficient as predicted by the KM-SUB model at 50 % RH (using the Zobrist et al.
 351 (2011) H₂O diffusion coefficients) was $\gamma = 0.06$ compared to $\gamma = 0.11$ at pH 5 and $\gamma = 0.21$ at pH 7. The
 352 reason for this strong dependence upon pH has been discussed previously and is due to the partitioning
 353 of HO₂ with its conjugate base O₂⁻, as shown by Reaction 4, affecting the effective Henry's law
 354 coefficient and the effective rate constants (Thornton et al., 2008). Although it was not possible to
 355 measure the actual pH of the aerosol particles, it was possible to estimate the concentration of copper

356 (II) sulphate (which is a weak acid) within the aerosol particles using the known growth factors of
357 sucrose aerosol particles (Lu et al., 2014). The pH of 0.05 M and 0.1 M copper (II) sulphate solutions
358 (which were calculated to be the extremes of the possible copper concentrations over the RH range)
359 were then measured using a pH meter (Jenway, 3310) as being in the range of 4.10 ± 0.05 . It is expected
360 that the pH would be dominated by the presence of copper sulfate rather than sucrose which has a pH
361 of 7 in water and a very high pKa of 12.6. Therefore, there is confidence that the correct initial aerosol
362 pH was inputted into the model. Hence, while the HO₂ uptake coefficient might depend on further
363 factors such as aerosol pH, a clear dependence on relative humidity, and hence particle viscosity could
364 be observed, and it remains likely that at low humidity a surface loss process becomes dominating.

365

366 **HO₂ uptake by SOA**

367

368 A summary of all HO₂ uptake experiments performed on SOA is shown in Table 2. On average
369 the HO₂ uptake coefficient was measured as 0.004 ± 0.002 onto TMB derived aerosol particles produced
370 in the PAM chamber, whereas for α -pinene derived aerosol particles only an upper limit of 0.001
371 (obtained from the error in the slope of Figure 4(a)) could be placed on the HO₂ uptake coefficient at
372 50 and 80 % RH. It should be noted that for the α -pinene experiments the HO₂ uptake coefficient was
373 non-measurable for both ozonolysis and photochemistry experiments using both the smog chamber and
374 the PAM chamber as sources of the SOA, and therefore only upper limits of individual experiments are
375 reported in

376

377 Table 2. There was some variability for the upper limits that were measured for individual α -
378 pinene experiments which is likely to be due to the maximum aerosol surface-to-volume ratio that was
379 obtained in each experiment.

380 There are several possible reasons for the larger HO₂ uptake coefficients being measured for
381 the TMB derived aerosol particles compared to the α -pinene derived aerosol particles. These reasons
382 will be summarised below, but include a differing particle viscosity, a different particle liquid water
383 content or a HO₂ + RO₂ reaction occurring within the aerosol particles. Although the viscosity of α -
384 pinene derived aerosol has been measured as $\sim 10^3$ Pa s at 70 % RH and $> 10^9$ Pa s for RH < 30 %, to
385 our knowledge, there are currently no measurements of the viscosity of TMB derived aerosol published
386 in the literature (Renbaum-Wolff et al., 2013). By running the KM-SUB model it can be estimated that
387 the diffusion coefficient of HO₂ within the particles would need to be approximately 1×10^{-10} cm² s⁻¹ for
388 TMB derived aerosol particles and $< 5 \times 10^{-12}$ cm² s⁻¹ for α -pinene derived aerosol particles. This range

389 of values seems to be consistent with the diffusion coefficients estimated by Berkemeier et al. (2014)
390 and Lienhard et al. (2015) for water diffusion in low and medium O:C SOA.

391 Thornton et al. (2003) previously suggested that for malonic acid aerosol particles the liquid
392 water content could be limiting the aqueous chemistry below 40 % RH. As can be seen by the HO₂
393 reaction scheme, the rate of Reaction R6 is dependent upon the liquid water concentration within the
394 aerosol, and therefore the uptake coefficient could be limited by a low aerosol liquid water content.
395 However, there remains some uncertainty as to whether the liquid water content of TMB derived aerosol
396 particles would be higher than the liquid water content of α -pinene derived aerosol particles. Duplissy
397 et al. (2011) measured a higher hygroscopicity parameter (κ_{org}) for TMB derived aerosol particles
398 compared to α -pinene derived aerosol particles whereas Lambe et al. (2011b) and Berkemeier et al.
399 (2014) stated the opposite. However, as well as being dependent upon the hygroscopicity parameter,
400 the liquid water content of the aerosol particles would also be dependent upon the O:C ratio in the SOA.

401 If the viscosity and liquid water content of the α -pinene and TMB derived aerosol particles are
402 similar, the larger HO₂ uptake coefficients measured for TMB derived aerosol particles could be due to
403 a higher reactivity of these aerosol particles towards HO₂. This could be the case if the TMB derived
404 aerosol particles contained reactive radical species such as organic peroxy radicals, RO₂, which partition
405 into the aerosol or are formed within the aerosols by intra-particle reactions (Donahue et al., 2012; Lee
406 et al., 2016). As previously stated in the Data Analysis section, during α -pinene experiments, no
407 indication of RO₂ being present in the flow tube was observed by FAGE as a HO₂ interference.
408 However, for TMB derived aerosol particles, a large background signal was observed by FAGE
409 indicating that reactive radical species were likely to be present within the flow tube. If the reaction of
410 HO₂ with these species at the surface or within the bulk of the aerosol was faster than the equivalent
411 gas phase reaction, a larger HO₂ uptake coefficient would be observed.

412

413 **Atmospheric implications and conclusions**

414

415 The effect of aerosol viscosity upon HO₂ uptake coefficients was systematically investigated
416 with a combination of HO₂ uptake coefficient measurements and a state-of-the-art kinetic model. A
417 good correlation was obtained between measured HO₂ uptake coefficients onto copper doped sucrose
418 aerosols as a function of RH and the KM-SUB model output. At higher relative humidities the uptake
419 was limited by mass accommodation whilst at lower relative humidities the aerosol particles were
420 viscous and the uptake was limited by surface reaction. These results imply that viscous aerosol particles
421 will have very little impact upon gaseous tropospheric HO₂ concentrations.

422 The first measurements of the HO₂ uptake coefficient onto SOA have been reported in this
423 work. The HO₂ uptake coefficient measured for α-pinene derived aerosol particles was below the limit
424 of detection of the apparatus ($\gamma < 0.001$) whereas for TMB derived aerosol particles the uptake
425 coefficient was measurable ($\gamma = 0.004 \pm 0.002$). These results are consistent with the copper doped
426 sucrose results, and indicate that the impact of SOA on gaseous HO₂ concentrations would likely be
427 small. However, it remains unclear as to the reasons for the larger HO₂ uptake coefficient measured
428 onto TMB derived aerosol particles compared to α-pinene derived aerosol particles. The possibility that
429 the larger uptake coefficient onto TMB derived aerosol particles was due to a lower viscosity of the
430 aerosol particles or a higher liquid water content compared to α-pinene derived aerosol particles cannot
431 be confirmed until further measurements of the viscosity and liquid water content of TMB derived
432 aerosol particles are published in the literature. However, if the larger uptake coefficients are due to a
433 HO₂ + RO₂ reaction within the aerosol, this could impact the HO₂ uptake coefficient for any aerosol
434 containing RO₂. The actual increase would depend on a variety of factors such as the concentrations of
435 RO₂, the partition coefficients of RO₂ to the aerosol particles, the reactivity of different RO₂ species
436 with HO₂ radicals and the intra-particle formation of RO₂ and other reactive radicals (Lee et al.,
437 2016;Donahue et al., 2012;Tong et al., 2016). The HO₂ + RO₂ reaction could potentially occur within
438 the majority of aerosol particles within the atmosphere, this could have implications for the gaseous
439 HO₂ and RO₂ concentrations in the troposphere which could then impact upon the concentrations of
440 other species such as ozone.

441

442 **Acknowledgements**

443

444 PSJL is grateful to NERC for the award of a studentship. LKW and DEH are also grateful to the NERC
445 funded National Centre for Atmospheric Science for ongoing support and to NERC for funding of the
446 HO₂ aerosol uptake apparatus (grant reference NE/F020651/1). TB was supported by the Max Planck
447 Graduate Center with the Johannes Gutenberg-Universität Mainz (MPGC). The experiments at PSI
448 were supported by T. Bartels-Rausch and M. Birrer. MA and MK were supported by the Swiss National
449 Science Foundation (grant nos 149492, CR3213-140851).

450

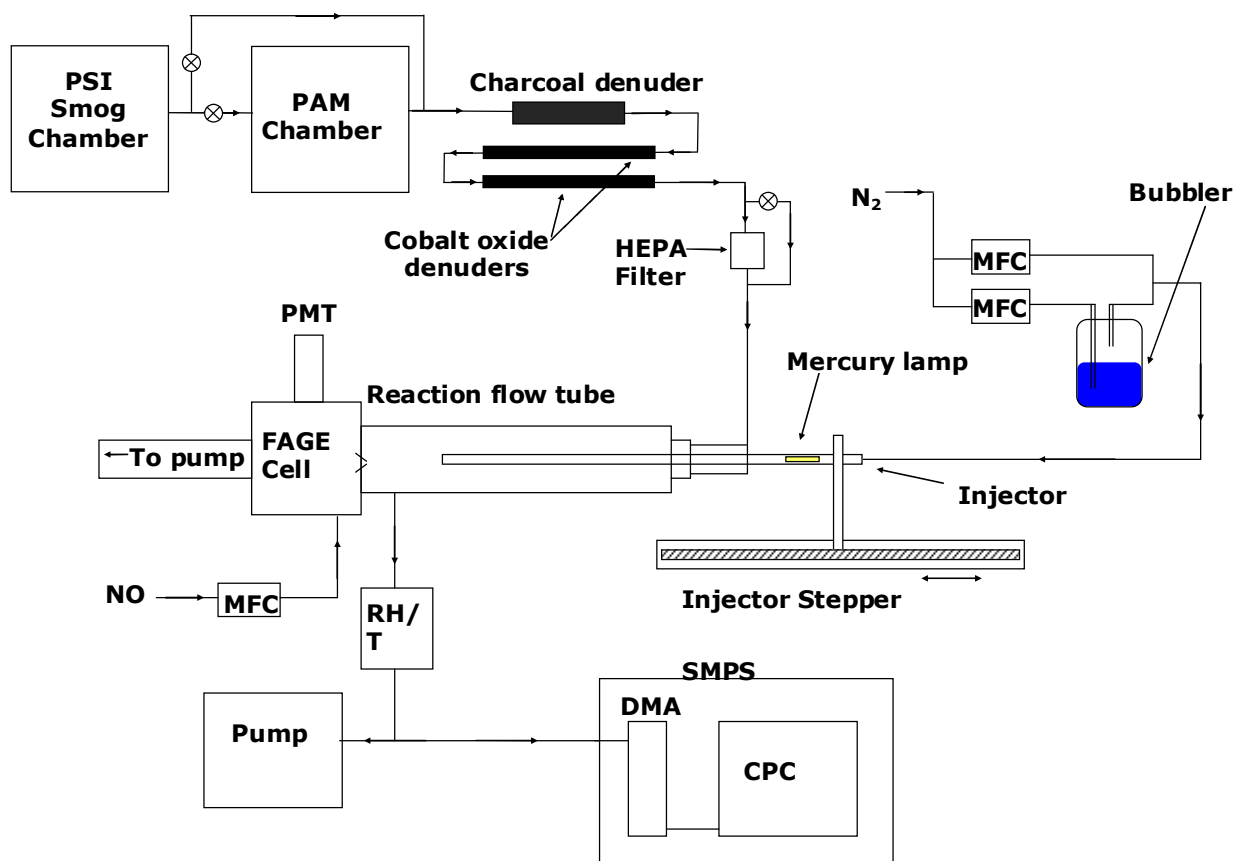
451

452

453

454

455 **Figures**



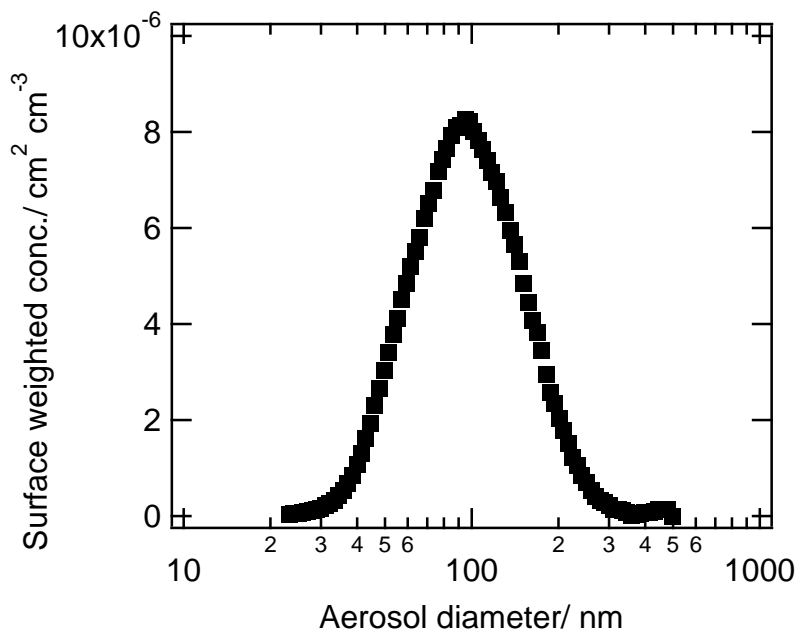
456

457 **Figure 1:** A schematic of the experimental setup used to measure HO₂ uptake coefficients onto SOA
 458 aerosol particles. Key: PAM- Potential aerosol mass, PMT- Photomultiplier tube, FAGE-
 459 Fluorescence Assay by Gas Expansion, MFC- Mass flow controller, RH/ T- relative humidity and
 460 temperature probe, SMPS- Scanning mobility particle sizer, DMA- Differential mobility analyser,
 461 CPC- Condensation particle counter.

462

463

464



465

466 **Figure 2:** An example of the size distribution for α -pinene derived aerosol particles formed in the
 467 PAM chamber at a relative humidity of ~ 50 %.

468

469

470

471

472

473

474

475

476

477

478

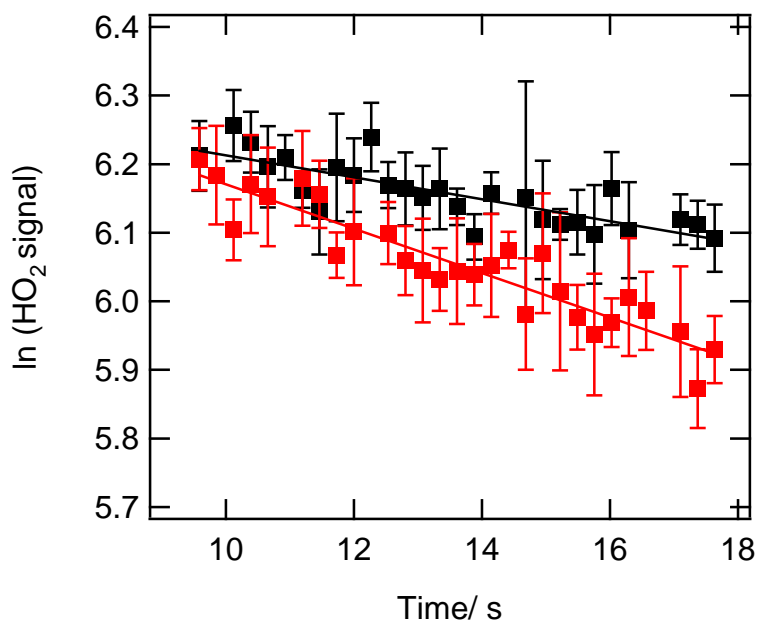
479

480

481

482

483



484

485 **Figure 3:** Examples of the HO₂ wall loss without any aerosol particles along the flow tube (black
 486 squares) and the HO₂ loss with an aerosol surface area of $2.2 \times 10^{-4} \text{ cm}^2 \text{ cm}^{-3}$ for TMB derived aerosol
 487 particles at an initial HO₂ concentration of $\sim 1 \times 10^9 \text{ molecule cm}^{-3}$ (red squares) and for RH = 50 %.
 488 The error bars represent one standard deviation in the measured HO₂ signal for a measurement time per
 489 point of 3 seconds.

490

491

492

493

494

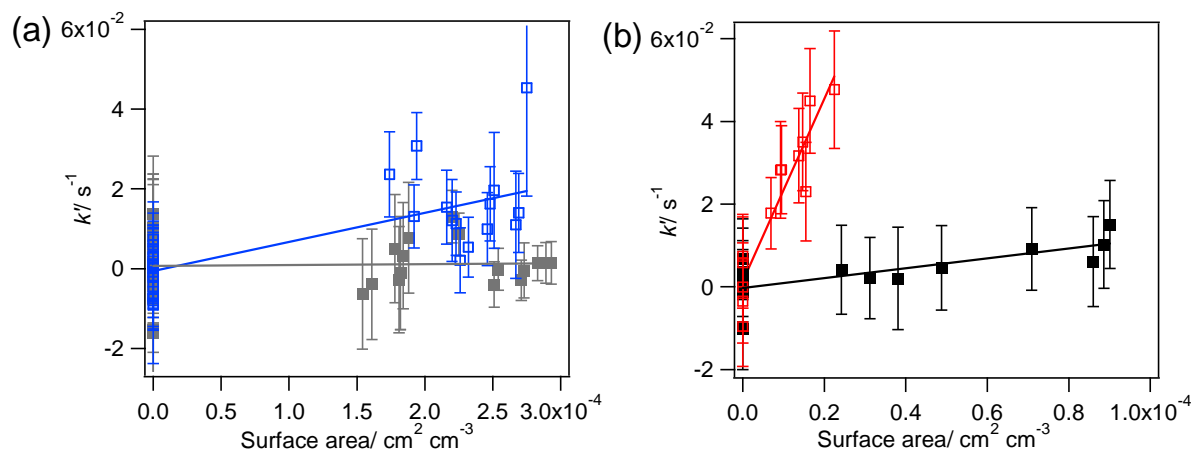
495

496

497

498

499



500

501

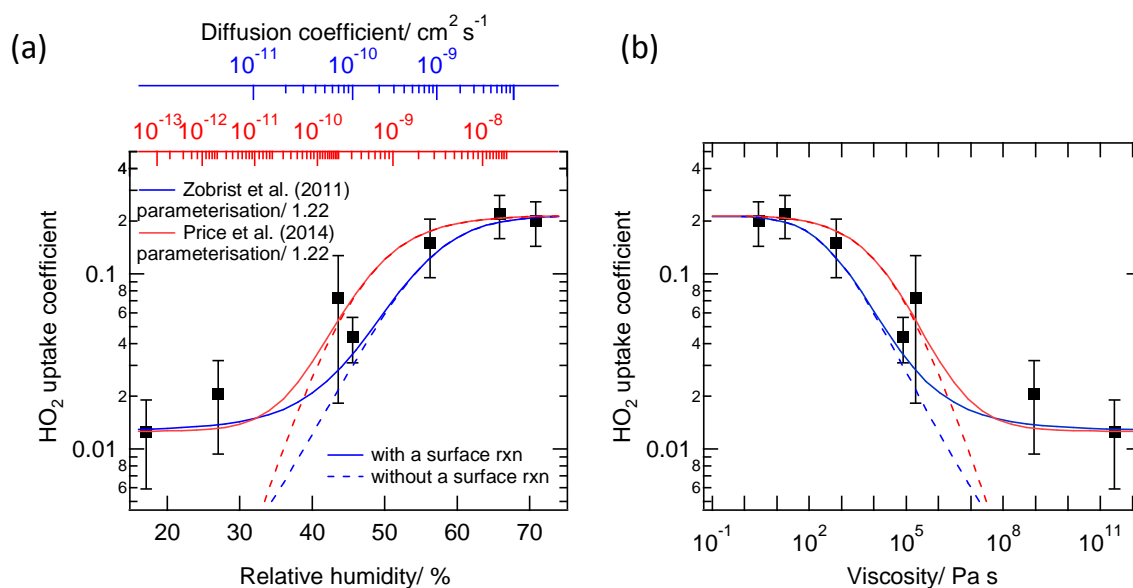
502 **Figure 4:** The pseudo-first-order rate constants with the wall losses subtracted as a function of aerosol
 503 surface area for (a) α -pinene derived aerosol particles (grey) and TMB derived aerosol particles (blue)
 504 at 50 % RH and a pressure of 904 – 929 mbar and (b) copper doped sucrose aerosol particles at 17%
 505 RH (black) and 71% RH (red) at atmospheric pressure. Experiments were performed at 293 ± 2 K. In
 506 panel (a) experiments were performed using the PAM chamber as the source of aerosol particles and
 507 represent experiments 5 and 6 in Table 2. Error bars represent the 1 standard deviation propagated
 508 uncertainty for individual determinations of k' . The data points at an aerosol surface area of $0 \text{ cm}^2 \text{ cm}^{-3}$
 509 (no aerosol particles present) are repeats of the wall loss decays taken throughout the experiment and
 510 are within error of each other.

511

512

513

514



516

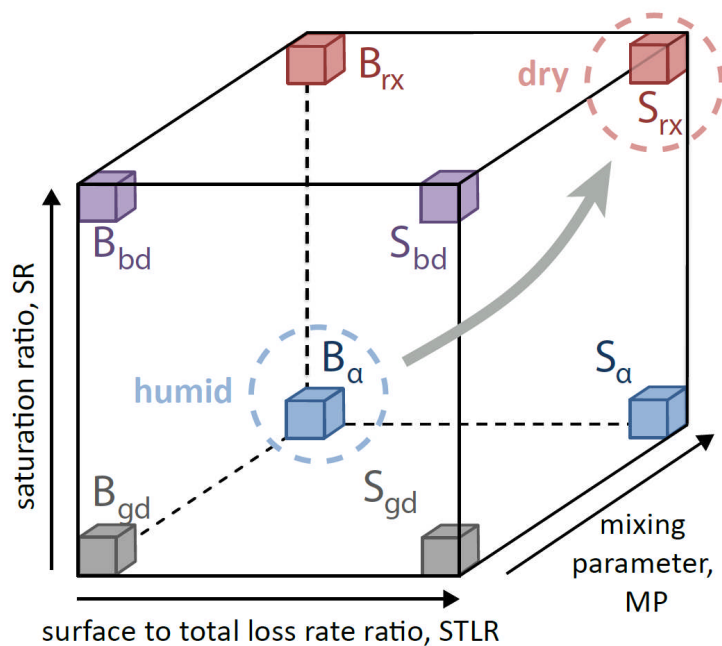
517 **Figure 5:** The HO_2 uptake coefficient onto copper (II) doped sucrose aerosol particles as a function of
 518 (a) relative humidity and (b) aerosol particle viscosity. The lines represent the expected HO_2 uptake
 519 coefficient calculated using the KM-SUB model using the Price et al. (2014) (red) and Zobrist et al.
 520 (2011) (blue) diffusion parameterisations (see model description section) and with (solid) and without
 521 (dashed) the inclusion of a surface reaction (Reaction R11). The viscosity within sucrose aerosol
 522 particles is based upon the data and fitting shown in Power et al. (2013) and Marshall et al. (2016)
 523 whilst the red and blue axes in panel (a) are the Price et al. (2014) and Zobrist et al. (2011) diffusion
 524 parameterisations, respectively. The error bars represent two standard deviations of the propagated error
 525 in the gradient of the k' against aerosol surface area graphs.

526

527

528

529



530

531 **Figure 6:** The kinetic cube representing the eight limiting cases for uptake of gases to aerosol particles
 532 (Berkemeier et al., 2013). B_{rx} : bulk reaction limited by chemical reaction, B_{bd} : bulk reaction limited by
 533 bulk diffusion of the volatile reactant and the condensed reactant, B_{α} : bulk reaction limited by mass
 534 accommodation, B_{gd} : bulk reaction limited by gas-phase diffusion; S_{rx} : surface reaction limited by
 535 chemical reaction, S_{bd} : surface reaction limited by bulk diffusion of a condensed reactant, S_{α} : surface
 536 reaction limited by surface accommodation, S_{gd} : surface reaction limited by gas-phase diffusion. For
 537 copper doped sucrose aerosol particles, the HO_2 uptake coefficient is limited by mass accommodation
 538 under humid conditions and by chemical reaction at the surface at low relative humidity.

539

540

541

542

543

544

545

546

547

548

549

550

551 **Tables**

552

553 **Table 1:** The parameters used in the KM-SUB HO₂ uptake model over all relative humidities.

Parameter	Description	Value at 293 K	Reference
$k_{BR,1}$	Rate constant, R5	$1.3 \times 10^{-15} \text{ cm}^3 \text{ s}^{-1}$	Thornton et al. (2008)
$k_{BR,2}$	Rate constant, R6	$1.5 \times 10^{-13} \text{ cm}^3 \text{ s}^{-1}$	Thornton et al. (2008)
$k_{BR,3}$	Rate constant, R7	$1.7 \times 10^{-13} \text{ cm}^3 \text{ s}^{-1}$	Jacob (2000)
$k_{BR,4}$	Rate constant, R8	$1.3 \times 10^{-11} \text{ cm}^3 \text{ s}^{-1}$	Jacob (2000)
$k_{BR,5}$	Rate constant, R9	$2.5 \times 10^{-12} \text{ cm}^3 \text{ s}^{-1}$	Jacob (2000)
$k_{BR,6}$	Rate constant, R10	$1.6 \times 10^{-11} \text{ cm}^3 \text{ s}^{-1}$	Jacob (2000)
k_{GP}	Rate constant, R3	$3 \times 10^{-12} \text{ cm}^3 \text{ s}^{-1}$	Sander et al. (2003)
K_{eq}	Equilibrium constant, R4	$2.1 \times 10^{-5} \text{ M}$	Thornton et al. (2008)
H_{HO_2}	HO ₂ Henry's law constant	5600 M atm^{-1}	Thornton et al. (2008)
τ_d	HO ₂ desorption lifetime	$1.5 \times 10^{-3} \text{ s}$	Shiraiwa et al. (2010)
$\alpha_{s,0}$	HO ₂ surface accommodation at time 0	0.22	
D_{g,HO_2}	HO ₂ gas phase diffusion rate constant	$0.25 \text{ cm}^2 \text{ s}^{-1}$	Thornton et al. (2008)
[Cu]	Copper concentration (used when modelling copper doped sucrose aerosol particles)	$5 \times 10^{19} \text{ cm}^{-3}$	
T	Temperature	293 K	

554

555

556

557

558

559

560

561

562 **Table 2:** Summary of the reactants and conditions that were utilised and the HO₂ uptake coefficients
 563 that were measured during the experiments. Experiments 1 - 4 were performed using the smog
 564 chamber whereas experiments 5 - 9 utilised the PAM chamber.
 565

Experiment number	Reaction type	Initial precursor concentrations	UV	Relative humidity in the chamber/%	Pressure in the flow tube/mbar	Maximum aerosol surface to volume ratio in the flow tube/cm ² cm ⁻³	HO ₂ uptake coefficient (γ)
1	α-pinene ozonolysis	[α-pinene] = 600 ppb [O ₃] = 280 ppb	Off	50	987	6.30 × 10 ⁻⁵	< 0.01
2	α-pinene ozonolysis	[α-pinene] = 600 ppb [O ₃] = 280 ppb	Off	50	965	1.30 × 10 ⁻⁴	< 0.004
3	α-pinene ozonolysis	[α-pinene] = 200 ppb [O ₃] = 310 ppb	Off	80	939	7.10 × 10 ⁻⁵	< 0.006
4	α-pinene photochemistry	[α-pinene] = 500 ppb [NO ₂] = 350 ppb	On	50	940	6.30 × 10 ⁻⁵	< 0.018
5	α-pinene photochemistry	[α-pinene] = 500 ppb	On	50	929	2.93 × 10 ⁻⁴	< 0.001
6	TMB photochemistry	[TMB] = 2 ppm	On	50	923	2.75 × 10 ⁻⁴	0.004 ± 0.002
7	TMB photochemistry	[TMB] = 2ppm	On	50	918	2.32 × 10 ⁻⁴	0.004 ± 0.003
8	α-pinene photochemistry	[α-pinene] = 500 ppb	On	50	927	1.88 × 10 ⁻⁴	< 0.005
9	α-pinene photochemistry	[α-pinene] = 1 ppm	On	80	904	3.90 × 10 ⁻⁴	< 0.001

566

567

568

569

570

571

572 **References**

- 573 Ammann, M.: Using ^{13}N as tracer in heterogeneous atmospheric chemistry experiments,
574 *Radiochimica Acta International journal for chemical aspects of nuclear science and technology*, 89,
575 831, 2001.
- 576 Arens, F., Gutzwiller, L., Baltensperger, U., Gäggeler, H. W., and Ammann, M.: Heterogeneous
577 reaction of NO_2 on diesel soot particles, *Environ. Sci. Technol.*, 35, 2191-2199, 2001.
- 578 Badger, C. L., Griffiths, P. T., George, I., Abbatt, J. P. D., and Cox, R. A.: Reactive uptake of N_2O_5
579 by aerosol particles containing mixtures of humic acid and ammonium sulfate, *J. Phys. Chem. A*, 110,
580 6986-6994, 10.1021/jp0562678, 2006.
- 581 Bedjanian, Y., Romanias, M. N., and El Zein, A.: Uptake of HO_2 radicals on Arizona Test Dust,
582 *Atmos. Chem. Phys.*, 6461-6471, 2013.
- 583 Behr, P., Scharfenort, U., Ataya, K., and Zellner, R.: Dynamics and mass accommodation of HCl
584 molecules on sulfuric acid–water surfaces, *Phys. Chem. Chem. Phys.*, 11, 8048-8055, 2009.
- 585 Berkemeier, T., Huisman, A. J., Ammann, M., Shiraiwa, M., Koop, T., and Pöschl, U.: Kinetic
586 regimes and limiting cases of gas uptake and heterogeneous reactions in atmospheric aerosols and
587 clouds: a general classification scheme, *Atmos. Chem. Phys.*, 13, 6663-6686, 2013.
- 588 Berkemeier, T., Shiraiwa, M., Pöschl, U., and Koop, T.: Competition between water uptake and ice
589 nucleation by glassy organic aerosol particles, *Atmos. Chem. Phys.*, 14, 12513-12531, 2014.
- 590 Berkemeier, T., Steimer, S. S., Krieger, U. K., Peter, T., Pöschl, U., Ammann, M., and Shiraiwa, M.:
591 Ozone uptake on glassy, semi-solid and liquid organic matter and the role of reactive oxygen
592 intermediates in atmospheric aerosol chemistry, *Phys. Chem. Chem. Phys.*, 18, 12662-12674, 2016.
- 593 Bones, D. L., Reid, J. P., Lienhard, D. M., and Krieger, U. K.: Comparing the mechanism of water
594 condensation and evaporation in glassy aerosol, *P. Natl. Acad. Sci.*, 109, 11613-11618,
595 10.1073/pnas.1200691109, 2012.
- 596 Brown, R. L.: Tubular Flow Reactors With 1st-Order Kinetics, *J. Res. Nat. Bur. Stand.*, 83, 1-8,
597 1978.
- 598 Bruns, E., El Haddad, I., Keller, A., Klein, F., Kumar, N., Pieber, S., Corbin, J., Slowik, J., Brune, W.,
599 and Baltensperger, U.: Inter-comparison of laboratory smog chamber and flow reactor systems on
600 organic aerosol yield and composition, *Atmospheric Measurement Techniques*, 8, 2315-2332, 2015.
- 601 Calvert, J. G., Atkinson, R., Becker, K. H., Kamens, R. M., Seinfeld, J. H., Wallington, T. J., and
602 Yarwood, G.: *The Mechanisms of Atmospheric Oxidation of Aromatic Hydrocarbons*, Oxford
603 University Press, Oxford, 2002.
- 604 Champion, D., Hervet, H., Blond, G., Le Meste, M., and Simatos, D.: Translational diffusion in
605 sucrose solutions in the vicinity of their glass transition temperature, *J. Phys. Chem. B*, 101, 10674-
606 10679, 1997.
- 607 Davidovits, P., Kolb, C. E., Williams, L. R., Jayne, J. T., and Worsnop, D. R.: Mass accommodation
608 and chemical reactions at gas-liquid interfaces, *Chem. Rev.*, 106, 1323-1354, 10.1021/cr040366k,
609 2006.
- 610 Davies, J. F., and Wilson, K. R.: Nanoscale interfacial gradients formed by the reactive uptake of OH
611 radicals onto viscous aerosol surfaces, *Chem. Sci.*, 6, 7020-7027, 2015.

612 Donahue, N. M., Henry, K. M., Mentel, T. F., Kiendler-Scharr, A., Spindler, C., Bohn, B., Brauers,
613 T., Dorn, H. P., Fuchs, H., and Tillmann, R.: Aging of biogenic secondary organic aerosol via gas-
614 phase OH radical reactions, *P. Natl. Acad. Sci.*, 109, 13503-13508, 2012.

615 Duplissy, J., DeCarlo, P. F., Dommen, J., Alfarra, M. R., Metzger, A., Barmapadimos, I., Prevot, A. S.
616 H., Weingartner, E., Tritscher, T., Gysel, M., Aiken, A. C., Jimenez, J. L., Canagaratna, M. R.,
617 Worsnop, D. R., Collins, D. R., Tomlinson, J., and Baltensperger, U.: Relating hygroscopicity and
618 composition of organic aerosol particulate matter, *Atmos. Chem. Phys.*, 11, 1155-1165, 10.5194/acp-
619 11-1155-2011, 2011.

620 Fowler, D., Pilegaard, K., Sutton, M., Ambus, P., Raivonen, M., Duyzer, J., Simpson, D., Fagerli, H.,
621 Fuzzi, S., and Schjørring, J. K.: Atmospheric composition change: ecosystems–atmosphere
622 interactions, *Atmos. Environ.*, 43, 5193-5267, 2009.

623 Fuchs, H., Bohn, B., Hofzumahaus, A., Holland, F., Lu, K. D., Nehr, S., Rohrer, F., and Wahner, A.:
624 Detection of HO₂ by laser-induced fluorescence: calibration and interferences from RO₂ radicals,
625 *Atmos. Meas. Tech.*, 4, 1209-1225, 10.5194/amt-4-1209-2011, 2011.

626 Fuchs, N. A., and Sutugin, A. G.: Properties of Highly Dispersed Aerosols, in, 1970.

627 George, I. J., Matthews, P. S. J., Whalley, L. K., Brooks, B., Goddard, A., Baeza-Romero, M. T., and
628 Heard, D. E.: Measurements of uptake coefficients for heterogeneous loss of HO₂ onto submicron
629 inorganic salt aerosols, *Phys. Chem. Chem. Phys.*, 15, 12829-12845, 10.1039/C3CP51831K, 2013.

630 Gržinić, G., Bartels-Rausch, T., Berkemeier, T., Türler, A., and Ammann, M.: Viscosity controls
631 humidity dependence of N₂O₅ uptake to citric acid aerosol, *Atmos. Chem. Phys.*, 15, 13615-13625,
632 2015.

633 Hanson, D. R., Ravishankara, A., and Solomon, S.: Heterogeneous reactions in sulfuric acid aerosols:
634 A framework for model calculations, *J. Geophys. Res. - Atmos.*, 99, 3615-3629, 1994.

635 Heard, D. E., and Pilling, M. J.: Measurement of OH and HO₂ in the troposphere, *Chem. Rev.*, 103,
636 5163-5198, 10.1021/cr020522s, 2003.

637 Houle, F., Hinsberg, W., and Wilson, K.: Oxidation of a model alkane aerosol by OH radical: the
638 emergent nature of reactive uptake, *Phys. Chem. Chem. Phys.*, 17, 4412-4423, 2015.

639 Jacob, D. J.: Heterogeneous chemistry and tropospheric ozone, *Atmos. Environ.*, 34, 2131-2159,
640 2000.

641 Kanakidou, M., Seinfeld, J. H., Pandis, S. N., Barnes, I., Dentener, F. J., Facchini, M. C., Van
642 Dingenen, R., Ervens, B., Nenes, A., Nielsen, C. J., Swietlicki, E., Putaud, J. P., Balkanski, Y., Fuzzi,
643 S., Horth, J., Moortgat, G. K., Winterhalter, R., Myhre, C. E. L., Tsigaridis, K., Vignati, E.,
644 Stephanou, E. G., and Wilson, J.: Organic aerosol and global climate modelling: a review, *Atmos.*
645 *Chem. Phys.*, 5, 1053-1123, 2005.

646 Kanaya, Y., Cao, R., Kato, S., Miyakawa, Y., Kajii, Y., Tanimoto, H., Yokouchi, Y., Mochida, M.,
647 Kawamura, K., and Akimoto, H.: Chemistry of OH and HO₂ radicals observed at Rishiri Island,
648 Japan, in September 2003: Missing daytime sink of HO₂ and positive nighttime correlations with
649 monoterpenes, *J. Geophys. Res. - Atmos.*, 112, D11308, 10.1029/2006jd007987, 2007.

650 Kang, E., Root, M. J., Toohey, D. W., and Brune, W. H.: Introducing the concept of Potential Aerosol
651 Mass (PAM), *Atmos. Chem. Phys.*, 7, 5727-5744, 2007.

652 Lakey, P. S. J., George, I. J., Whalley, L. K., Baeza-Romero, M. T., and Heard, D. E.: Measurements
653 of the HO₂ Uptake Coefficients onto Single Component Organic Aerosols, *Environ. Sci. Tech.*,
654 10.1021/acs.est.5b00948, 2015a.

655 Lakey, P. S. J., George, I. J., Baeza-Romero, M. T., Whalley, L. K., and Heard, D. E.: Organics
656 substantially reduce HO₂ uptake onto aerosols containing transition metal ions, *J. Phys Chem. A*,
657 2015b.

658 Lambe, A., Ahern, A., Williams, L., Slowik, J., Wong, J., Abbatt, J., Brune, W., Ng, N., Wright, J.,
659 and Croasdale, D.: Characterization of aerosol photooxidation flow reactors: heterogeneous oxidation,
660 secondary organic aerosol formation and cloud condensation nuclei activity measurements,
661 *Atmospheric Measurement Techniques*, 4, 445-461, 2011a.

662 Lambe, A. T., Onasch, T. B., Massoli, P., Croasdale, D. R., Wright, J. P., Ahern, A. T., Williams, L.
663 R., Worsnop, D. R., Brune, W. H., and Davidovits, P.: Laboratory studies of the chemical
664 composition and cloud condensation nuclei (CCN) activity of secondary organic aerosol (SOA) and
665 oxidized primary organic aerosol (OPOA), *Atmos. Chem. Phys.*, 11, 8913-8928, 10.5194/acp-11-
666 8913-2011, 2011b.

667 Lee, B. H., Mohr, C., Lopez-Hilfiker, F. D., Lutz, A., Hallquist, M., Lee, L., Romer, P., Cohen, R. C.,
668 Iyer, S., and Kurtén, T.: Highly functionalized organic nitrates in the southeast United States:
669 Contribution to secondary organic aerosol and reactive nitrogen budgets, *P. Natl. Acad. Sci.*, 113,
670 1516-1521, 2016.

671 Lienhard, D., Huisman, A., Krieger, U., Rudich, Y., Marcolli, C., Luo, B., Bones, D., Reid, J., Lambe,
672 A., and Canagaratna, M.: Viscous organic aerosol particles in the upper troposphere: diffusivity-
673 controlled water uptake and ice nucleation?, *Atmos. Chem. Phys.*, 15, 13599-13613, 2015.

674 Lim, H. J., and Turpin, B. J.: Origins of primary and secondary organic aerosol in Atlanta: Results' of
675 time-resolved measurements during the Atlanta supersite experiment, *Environ. Sci. Technol.*, 36,
676 4489-4496, 10.1021/es0206487, 2002.

677 Lu, J. W., Rickards, A. M., Walker, J. S., Knox, K. J., Miles, R. E., Reid, J. P., and Signorell, R.:
678 Timescales of water transport in viscous aerosol: measurements on sub-micron particles and
679 dependence on conditioning history, *Phys. Chem. Chem. Phys.*, 16, 9819-9830, 10.1039/c3cp54233e,
680 2014.

681 Mao, J., Jacob, D. J., Evans, M. J., Olson, J. R., Ren, X., Brune, W. H., St Clair, J. M., Crouse, J. D.,
682 Spencer, K. M., Beaver, M. R., Wennberg, P. O., Cubison, M. J., Jimenez, J. L., Fried, A., Weibring,
683 P., Walega, J. G., Hall, S. R., Weinheimer, A. J., Cohen, R. C., Chen, G., Crawford, J. H.,
684 McNaughton, C., Clarke, A. D., Jaegle, L., Fisher, J. A., Yantosca, R. M., Le Sager, P., and Carouge,
685 C.: Chemistry of hydrogen oxide radicals (HO_x) in the Arctic troposphere in spring, *Atmos. Chem.*
686 *Phys.*, 10, 5823-5838, 10.5194/acp-10-5823-2010, 2010.

687 Marshall, F. H., Miles, R. E., Song, Y.-C., Ohm, P. B., Power, R. M., Reid, J. P., and Dutcher, C. S.:
688 Diffusion and reactivity in ultraviscous aerosol and the correlation with particle viscosity, *Chem. Sci.*,
689 2016.

690 Matthews, P. S. J., Baeza-Romero, M. T., Whalley, L. K., and Heard, D. E.: Uptake of HO₂ radicals
691 onto Arizona test dust particles using an aerosol flow tube, *Atmos. Chem. Phys.*, 14, 7397-7408,
692 10.5194/acpd-14-4229-2014, 2014.

693 Ortega, A. M., Hayes, P. L., Peng, Z., Palm, B. B., Hu, W., Day, D. A., Li, R., Cubison, M. J., Brune,
694 W. H., Graus, M., Warneke, C., Gilman, J. B., Kuster, W. C., de Gouw, J. A., and Jimenez, J. L.:
695 Real-time measurements of secondary organic aerosol formation and aging from ambient air in an

696 oxidation flow reactor in the Los Angeles area, *Atmos. Chem. Phys. Discuss.*, 2015, 21907-21958,
697 10.5194/acpd-15-21907-2015, 2015.

698 Paulsen, D., Dommen, J., Kalberer, M., Prévôt, A. S. H., Richter, R., Sax, M., Steinbacher, M.,
699 Weingartner, E., and Baltensperger, U.: Secondary Organic Aerosol Formation by Irradiation of 1,3,5-
700 Trimethylbenzene–NO_x–H₂O in a New Reaction Chamber for Atmospheric Chemistry and Physics,
701 *Environ. Sci. Technol.*, 39, 2668-2678, 10.1021/es0489137, 2005.

702 Pöschl, U., and Shiraiwa, M.: Multiphase Chemistry at the Atmosphere–Biosphere Interface
703 Influencing Climate and Public Health in the Anthropocene, *Chem. Rev.*, 115, 4440-4475, 2015.

704 Power, R., Simpson, S., Reid, J., and Hudson, A.: The transition from liquid to solid-like behaviour in
705 ultrahigh viscosity aerosol particles, *Chem. Sci.*, 4, 2597-2604, 2013.

706 Price, H. C., Murray, B. J., Mattsson, J., O'Sullivan, D., Wilson, T. W., Baustian, K. J., and Benning,
707 L. G.: Quantifying water diffusion in high-viscosity and glassy aqueous solutions using a Raman
708 isotope tracer method, *Atmos. Chem. Phys.*, 14, 3817-3830, 10.5194/acpd-13-29375-2013, 2014.

709 Qi, L., Nakao, S., and Cocker III, D. R.: Aging of secondary organic aerosol from α -pinene
710 ozonolysis: Roles of hydroxyl and nitrate radicals, *J. Air Waste Manage.*, 62, 1359-1369, 2012.

711 Renbaum-Wolff, L., Grayson, J. W., Bateman, A. P., Kuwata, M., Sellier, M., Murray, B. J., Shilling,
712 J. E., Martin, S. T., and Bertram, A. K.: Viscosity of alpha-pinene secondary organic material and
713 implications for particle growth and reactivity, *P. Natl. Acad. Sci.*, 110, 8014-8019,
714 10.1073/pnas.1219548110, 2013.

715 Sander, S. P., Friedl, R. R., Golden, D. M., Kurylo, M. J., Huie, R. E., Orkin, V. L., Moortgat, G. K.,
716 Ravishankara, A. R., Kolb, C. E., Molina, M. J., and Finlayson-Pitts, B. J.: *Chemical Kinetics and*
717 *Photochemical Data for Use in Atmospheric Studies*, JPL Publication, 14, 2003.

718 Schwartz, S., and Freiberg, J.: Mass-transport limitation to the rate of reaction of gases in liquid
719 droplets: Application to oxidation of SO₂ in aqueous solutions, *Atmos. Environ.*, 15, 1129-1144,
720 1981.

721 Shiraiwa, M., Pfrang, C., and Pöschl, U.: Kinetic multi-layer model of aerosol surface and bulk
722 chemistry (KM-SUB): the influence of interfacial transport and bulk diffusion on the oxidation of
723 oleic acid by ozone, *Atmos. Chem. Phys.*, 10, 3673-3691, 10.5194/acp-10-3673-2010, 2010.

724 Shiraiwa, M., Sosedova, Y., Rouvière, A., Yang, H., Zhang, Y., Abbatt, J. P., Ammann, M., and
725 Pöschl, U.: The role of long-lived reactive oxygen intermediates in the reaction of ozone with aerosol
726 particles, *Nature chemistry*, 3, 291-295, 2011a.

727 Shiraiwa, M., Ammann, M., Koop, T., and Pöschl, U.: Gas uptake and chemical aging of semisolid
728 organic aerosol particles, *P. Natl. Acad. Sci.*, 108, 11003-11008, 2011b.

729 Slade, J. H., and Knopf, D. A.: Multiphase OH oxidation kinetics of organic aerosol: The role of
730 particle phase state and relative humidity, *Geophys. Res. Lett.*, 41, 5297-5306, 2014.

731 Steimer, S., Lampimäki, M., Coz, E., Grzanic, G., and Ammann, M.: The influence of physical state
732 on shikimic acid ozonolysis: a case for in situ microspectroscopy, *Atmos. Chem. Phys.*, 14, 10761-
733 10772, 2014.

734 Steimer, S. S., Berkemeier, T., Gilgen, A., Krieger, U. K., Peter, T., Shiraiwa, M., and Ammann, M.:
735 Shikimic acid ozonolysis kinetics of the transition from liquid aqueous solution to highly viscous
736 glass, *Phys. Chem. Chem. Phys.*, 2015.

- 737 Stone, D., Whalley, L. K., and Heard, D. E.: Tropospheric OH and HO₂ radicals: field measurements
738 and model comparisons, *Chemical Society Reviews*, 41, 6348-6404, 10.1039/c2cs35140d, 2012.
- 739 Takahama, S., and Russell, L.: A molecular dynamics study of water mass accommodation on
740 condensed phase water coated by fatty acid monolayers, *J. Geophys. Res. - Atmos.*, 116, 2011.
- 741 Taketani, F., and Kanaya, Y.: Kinetics of HO₂ Uptake in Levoglucosan and Polystyrene Latex
742 Particles, *Journal of Physical Chemistry Letters*, 1, 1701-1704, 10.1021/jz100478s, 2010.
- 743 Taketani, F., Kanaya, Y., and Akimoto, H.: Kinetic Studies of Heterogeneous Reaction of HO₂
744 Radical by Dicarboxylic Acid Particles, *International Journal of Chemical Kinetics*, 45, 560-565,
745 10.1002/kin.20783, 2013.
- 746 Thornton, J. A., Braban, C. F., and Abbatt, J. P. D.: N₂O₅ hydrolysis on sub-micron organic aerosols:
747 the effect of relative humidity, particle phase, and particle size, *Phys. Chem. Chem. Phys.*, 5, 4593-
748 4603, 10.1039/B307498F, 2003.
- 749 Thornton, J. A., Jaegle, L., and McNeill, V. F.: Assessing known pathways for HO₂ loss in aqueous
750 atmospheric aerosols: Regional and global impacts on tropospheric oxidants, *J. Geophys. Res. -*
751 *Atmos.*, 113, D05303, 10.1029/2007jd009236, 2008.
- 752 Tong, H., Arangio, A. M., Lakey, P. S. J., Berkemeier, T., Liu, F., Kampf, C. J., Brune, W. H.,
753 Pöschl, U., and Shiraiwa, M.: Hydroxyl radicals from secondary organic aerosol decomposition in
754 water, *Atmos. Chem. Phys.*, 16, 1761-1771, 10.5194/acp-16-1761-2016, 2016.
- 755 Vieceli, J., Roeselova, M., Potter, N., Dang, L. X., Garrett, B. C., and Tobias, D. J.: Molecular
756 dynamics simulations of atmospheric oxidants at the air-water interface: Solvation and
757 accommodation of OH and O₃, *J. Phys. Chem. B*, 109, 15876-15892, 2005.
- 758 Whalley, L. K., Furneaux, K. L., Goddard, A., Lee, J. D., Mahajan, A., Oetjen, H., Read, K. A.,
759 Kaaden, N., Carpenter, L. J., Lewis, A. C., Plane, J. M. C., Saltzman, E. S., Wiedensohler, A., and
760 Heard, D. E.: The chemistry of OH and HO₂ radicals in the boundary layer over the tropical Atlantic
761 Ocean, *Atmos. Chem. Phys.*, 10, 1555-1576, 10.5194/acp-10-1555-2010, 2010.
- 762 Whalley, L. K., Blitz, M. A., Desservettaz, M., Seakins, P. W., and Heard, D. E.: Reporting the
763 sensitivity of laser-induced fluorescence instruments used for HO₂ detection to an interference from
764 RO₂ radicals and introducing a novel approach that enables HO₂ and certain RO₂ types to be
765 selectively measured, *Atmos. Meas. Tech.*, 6, 3425-3440, 10.5194/amt-6-3425-2013, 2013.
- 766 Zhou, S. M., Shiraiwa, M., McWhinney, R. D., Pöschl, U., and Abbatt, J. P. D.: Kinetic limitations in
767 gas-particle reactions arising from slow diffusion in secondary organic aerosol, *Faraday Discuss.*, 165,
768 391-406, 10.1039/c3fd00030c, 2013.
- 769 Zobrist, B., Soonsin, V., Luo, B. P., Krieger, U. K., Marcolli, C., Peter, T., and Koop, T.: Ultra-slow
770 water diffusion in aqueous sucrose glasses, *Phys. Chem. Chem. Phys.*, 13, 3514-3526,
771 10.1039/c0cp01273d, 2011.
- 772